1993

Impedance Spectroscopy as a Nondestructive Health Interrogation Tool for Lithium-BCX Cells

Branko N. Popov
University of South Carolina - Columbia, popov@engr.sc.edu

W. Zhang
University of South Carolina - Columbia

E. C. Darcy

Ralph E. White
University of South Carolina - Columbia, white@cec.sc.edu

Publication Info

Journal of the Electrochemical Society, 1993, pages 3097-3103.

10.1149/1.2220992
http://dx.doi.org/10.1149/1.2220992

Impedance Spectroscopy as a Nondestructive Health Interrogation Tool for Lithium-BCX Cells

B. N. Popov,* W. Zhang, E. C. Darcy,[a] and R. E. White*

Department of Chemical Engineering, University of South Carolina, Columbia, South Carolina 29208
[a]NASA-Johnson Space Center, Houston, Texas

ABSTRACT

The objective of this investigation was to study the growth of thick passivating layers on the Li anode in Li/BCX ($Li/SOCl_2$ + BrCl) cells which were stored for a period of 3 years. Impedance spectroscopy and equivalent circuit models were used to determine characterizing parameters for these cells. The equivalent circuit used for virgin cells includes a faradic contribution and diffusion of the electroactive species. The equivalent circuit for batteries stored 1 or 2 years includes the impedance of a metal/passive film interface, the resistance of the film, and the impedance of the passivating film/electrolyte interface. The equivalent circuit used for batteries stored for 3 years accounts for cathodic contributions in the overall impedance spectrum.

Lithium/$SOCl_2$ primary cells have long shelf lives because of the formation of a nonporous primary and porous secondary LiCl passivating films on the anode surface with high specific energy.[1-4] Unfortunately, the advantages available from these cells are affected by an excessive growth of this LiCl surface layer on the Li anode during long-term storage.[5-12] This surface layer is responsible for a voltage delay effect, which results in a cell voltage drop during the initial discharge.[13-17]

Improvements in the performance of the $Li/SOCl_2$ cell have been sought by the use of interhalogen compounds as additives. Krehl and Liang,[18] Liang *et al.*,[19] and Murphy *et al.*[20] reported that addition of BrCl to the $Li/SOCl_2$ resulted in a higher open-circuit voltage, higher capacity, better low temperature discharge performance, and some improved safety features. $Li/SOCl_2$ cells containing BrCl are popularly known as BCX cells. Abraham and Alamgir[21] studied the manner in which BrCl modifies the chemistry of the $Li/SOCl_2$ cell. They have shown, based on spectroscopic and cyclic voltammetric results, that reduction of BrCl in 1*M* $LiAlCl_4/SOCl_2$ proceeds via the reduction of Cl_2 and Br_2 prior to the reduction of $SOCl_2$. Abraham *et al.*[22] also reported that BrCl significantly modifies the chemistry of the $Li/SOCl_2$ cell. The LiBr formed appears to react with $SOCl_2$ to generate sulfur bromides, *e.g.*, (SO_2Br_2, Br_2) and LiCl. Sulfur halides are also formed in the cell by the reaction of Cl_2, BrCl, or Br_2 with S produced in the cell by the reduction of $SOCl_2$ which prevents the potentially explosive character of the lithium-sulfur combination.

Lithium/BCX cells are being considered for use by NASA in contingency and emergency applications. These applications stand to benefit greatly if the storage life of these cells can be expanded from the normal 2 year life-limit. Recent experiments conducted at NASA[23] on lithium/BCX cells show a significant decrease in capacity retention and a voltage delay when cells stored for five years were discharged at a rate less than the 30 h rate. It is suspected that the main reason for this is a significant increase in the cell internal impedance as a result of lithium electrode passivation.

Impedance spectroscopy (IS) has proved to be a powerful method for understanding interphase processes[24] and for characterizing the passive film which forms on the lithium electrode in primary batteries.[25-28] Using IS, Kuryakov *et al.*[29] studied the growth of the solid electrolyte film on a lithium anode as a function of storage time in $SOCl_2$ electrolyte. The film thickness on the anode exposed to the electrolyte for 125 days was calculated from the resistance of the solid electrolyte film and was determined to be 440 nm. Jamnik *et al.*[30-31] reported that the Cole-Cole distribution of relaxation times, by which the impedance response of the passive layer in $Li/SOCl_2$ batteries is described, can be regarded as the result of a position dependent resistivity of the film. Hughes *et al.*[32] studied the impedance of a BCX cell. They reported that the cell impedance is controlled mainly by the anode and that the very small interelectrode separation contributes to an erratic impedance behavior as charge is withdrawn from the cell.

The objective of this investigation was to determine the effectiveness of IS as a health interrogation tool for lithium/BCX cells and to characterize the passive film which forms on the lithium electrode.

Experimental

Lithium/BCX, D cells (Type P/N 3B21 manufactured by Wilson Greatbatch, Limited, Clarence, New York) were used. Their rated capacity is 14 Ah at 175 mA with a maximum current of 1 A. The cells are cylindrical with a diameter of 3.32 cm and a height of 5.80 cm. The lithium anode surface area is 146 cm^2.

The carbon cathode contained 93 weight percent (w/o) Shawinigan acetylene black (50% compressed) and 7 w/o Teflon binder (TFE-fluorocarbon resin dispersion No. 30, Du Pont). Each cell contained 44.5 g of electrolyte, comprised of 4.5 g of $LiAlCl_4$, 5.5 g of BrCl, and 34.5 g of $SOCl_2$. Details of the BCX cell are presented in Ref. 18 and 19.

Lithium/BCX cells, stored at 25°C from 15 to 20 days 1 year, 2 years, and 3 years (four of each) were obtained from the NASA-Johnson Space Center. No load checks were performed during storage at NASA nor after we received them. Since the cells were not exposed to any parasitic loads, we have assumed that the cells were all the same when they were new. Testing was carried out in our laboratory using ten representative cells for each year, and the results presented in this paper are average values of ten measurements.

IS data were obtained with a PAR Model 273 potentiostat/galvanostat and a PAR Model 5301A with a two-phase lock-in amplifier. Data were stored and analyzed using PAR M378 software on an IBM PC/2. The impedance spectra generally covered the frequency range from 0.01 Hz to 10 kHz with an ac voltage signal varying by ±5 mV, which ensured that the battery system was under minimum perturbation. The data were fit by using equivalent circuits and a nonlinear squares fitting program developed by Macdonald.[33]

Chemistry in the Li/BCX cell.—The open-circuit voltage (OCV) of the BCX cell is 3.92 V. According to Abraham *et al.*,[22] the observed higher OCV relative to that of a conventional $Li/SOCl_2$ cell (3.65 V) is due to the presence of Cl_2 resulting from the dissociation of BrCl into Br_2 and Cl_2

$$2BrCl \leftrightarrows Br_2 + Cl_2 \qquad [1]$$

Given that 5.5 g/liter: (0.048*M*) of BrCl contains 0.012*M* Cl_2 and 0.012*M* Br_2 in equilibrium with 0.024*M* BrCl and the degree of BrCl dissociation is 0.47, Abraham, *et al.*[22] com-

* Electrochemical Society Active Member.

puted that a virgin BCX cell contains 1.2 Ah BrCl, 0.6 Ah Br_2, and 0.6 Ah Cl_2.

The discharge of the BrCl in the cell proceeds through the reductions of Cl_2, Br_2, and BrCl [22]

$$Cl_2 + 2e \rightarrow 2Cl \quad \text{at} \quad -3.8\ V \qquad [2]$$

$$2BrCl + 2e^- \rightarrow 2Cl^- + Br_2 \quad \text{at} \quad -3.6\ V \qquad [3]$$

$$BrCl + 2e^- \rightarrow Br + Cl^- \quad \text{at} \quad -3.6\ V \qquad [4]$$

$$Br_2 + 2e \rightarrow 2Br^- \quad \text{at} \quad -3.6\ V \qquad [5]$$

Also, Li^+ reacts with Br^- to form LiBr which further reacts with $SOCl_2$ to form S, Br_2, SO_2, and LiCl. The S then reacts with Br_2 forming S_2Br_2. The Br_2 will also react with SO_2 forming SO_2Br_2. The overall reaction taking place in a $SOCl_2$/LiBr mixture may be summarized

$$2SOCl_2 + 4LiBr \rightarrow 4LiCl + SO_2Br_2 + \frac{1}{2}S_2Br_2 + \frac{1}{2}Br_2 \qquad [6]$$

By comparing the overall reactions in a Li/BCX cell and in a Li/$SOCl_2$, respectively

$$24Li + 8SOCl_2 + 8BrCl \rightarrow 24LiCl + 2SO_2Br_2 + 2SO_2 + 2S + S_2Br_2 + Br_2 \qquad [7]$$

$$4Li + 2SOCl_2 \rightarrow 4LiCl + S + SO_2 \qquad [8]$$

the main insoluble product of these reactions is LiCl. At the end of the discharge, Abraham *et al.*[22] suggested that Cl_2, Br_2, and BrCl react with S and SO_2 according to

$$Cl_2 + SO_2 \rightarrow SO_2Cl_2 \qquad [9]$$

$$S + Cl_2 \rightarrow SCl_2 \qquad [10]$$

$$4S + 2BrCl \rightarrow S_2Cl_2 + S_2Br_2 \qquad [11]$$

The sulfuryl halides and sulfur halides are probably reduced along with the reduction of $SOCl_2$.

Results and Discussion

During self-discharge of a Li/BCX battery, lithium reacts according to Eq. 7 to form a passive film on the Li electrode surface. A schematic representation of the nonporous primary and porous secondary films formed on the Li anode is presented in Fig. 1. Since the main insoluble product of reaction, Eq. 7, is LiCl, it is assumed in Fig. 1 that the passive film consists of LiCl crystals. However, sulfur halides, sulfuryl halides, and Br_2 formed during the self-discharge may also react with the Li anode causing anode passivation. The LiCl film grown thicker as time proceeds at a rate determined either by the transport of electronic charge from the Li primary layer interface to the LiCl primary layer/LiCl nonporous layer interface or by transport of Li^+ from the Li anode to the same interface. Since polarization from the equilibrium potential is controlled by ionic processes (the mobile electrons are the minority charge carriers in LiCl),[34,35] it is difficult to study the film growth on a Li anode by electrochemical techniques. In this study, the film growth rate was deduced by indirect measurement. The values of the LiCl film thickness for new

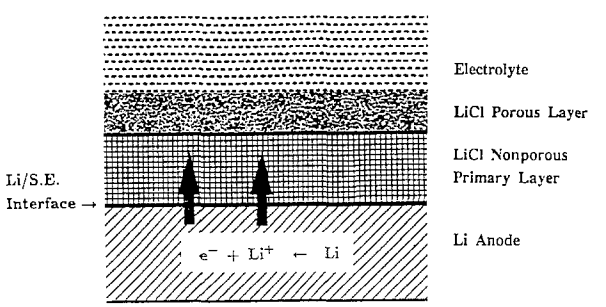

Fig. 1. Schematic representation of a passivated lithium anode in $SOCl_2$ solution at open circuit.

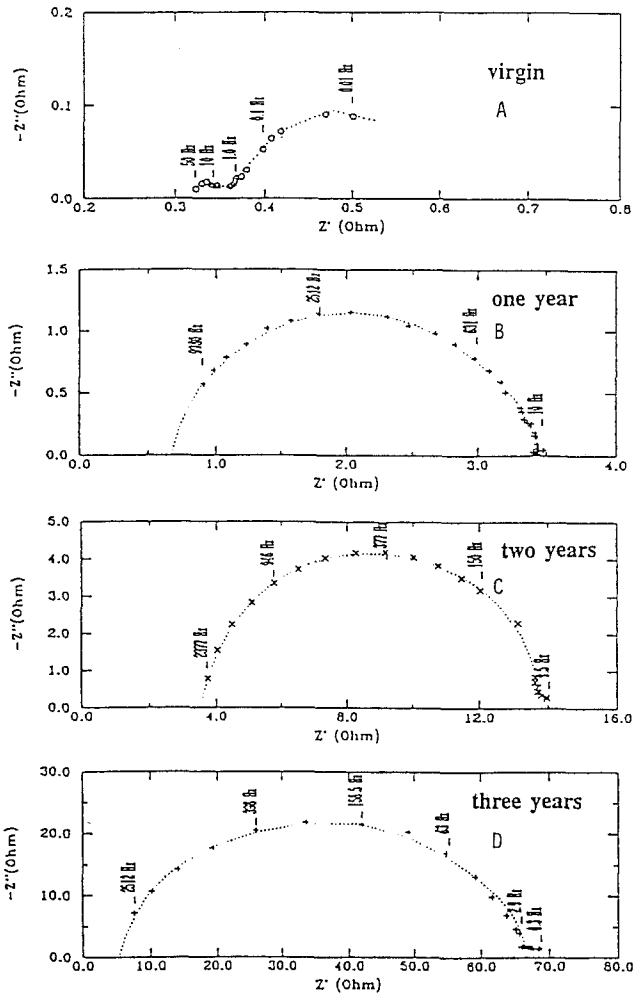

Fig. 2. Nyquist plots at OCV for Li/BCX cells at different ages: Virgin = 15-20 days old battery; B = 1 year; C = 2 years; D = 3 years.

lithium/BCX cells and for cells stored from 1 to 3 years were determined using IS.

Since the true area of the porous carbon electrode is much larger than the surface of the anode,[12-15] the cell impedance measured is assumed to be determined by the lithium anode. Accordingly, the main contribution to the impedance of the cell is made by the solid electrolyte, SE, (LiCl nonporous primary layer) present on the Li anode surface. Nyquist, Bode-magnitude, and Bode-phase plots were obtained at open-circuit potential for virgin cells (10 to 15 days old) and for cells stored 1, 2, and 3 years are shown in Fig. 2, 3, and 4, respectively. As seen in these figures, the formation of the passivating film on the anode causes an increase in the cells internal impedance and changes in the impedance diagrams. In Fig. 2A, the impedance spectrum of a virgin cell does not represent a fully equilibrated response. It consists of a small semicircle going off into a Warburg region which shows a return to real axis at frequencies lower than 0.01 Hz. For cells 15 to 20 days old, the LiCl passive film is not dense and completely established so the existence of holes and cracks in the film may be assumed through which the Li anode may be in contact with the electrolyte. The active surface area in such a case is $(1 - \theta)$, where θ is the area covered by the solid electrolyte. The corresponding diagram in the complex plane should give two loops, with resistances that are proportional to the active surface area of the lithium electrode. The small loop in Fig. 2A obtained at higher frequencies corresponds to a time constant due to the charge-transfer process and the double-layer capacitance. Since the Li anode passivation process is not separate from the charge-transfer process (lithium dissolution), the observed loop probably also reflects a passivation of the active surface

area. At low frequencies, 1.0-0.1 Hz, the Warburg line rises initially at an angle of approximately 45°. This is not close to the 22.5° angle expected for a porous electrode,[28] indicating the presence of a Li/electrolyte interface. As seen in Fig. 2A, the Warburg line starts to bend and returns to the real axis at lower frequencies. This phenomena was observed by Karunathilika *et al.*[34] and Hills *et al.*[35] who analyzed cells in which the distance between the anode and cathode is very small. According to these authors, this behavior is due to the effective distance between the electrodes being of the same order as $(D_i/\omega)^{1/2}$ at low frequencies, where D_i is the diffusion coefficient of the diffusing species i, and ω is the angular frequency of the perturbating signal.

The data presented in Fig. 2 were fit by using the equivalent circuits shown in Fig. 5 and a nonlinear, least squares fitting program. The results are presented as dotted curves in Fig. 2. The best fitting of the impedance data for cells which are 15 to 20 days old was obtained using the equivalent circuit shown in Fig. 5A, indicating that in the case of a virgin battery a noticeably dense passive film had not formed on the anode. Thus, the equivalent circuit accounts only for the faradaic contribution and for diffusion of the electroactive species. Using the equivalent circuit shown in Fig. 5A, the charge-transfer resistance (R_{ct}) had an average value of $5.82 \times 10^{-2}\ \Omega \pm 2.05 \times 10^{-2}\ \Omega$. This value was used to estimate i_o, the exchange current density

$$i_o = \frac{RT}{FR_{ct}a} \qquad [12]$$

where, at 25°C, the evaluated charge-transfer resistance value gives an anodic exchange current density of 0.003 A/cm^2, which is in agreement with the value of 0.002 A/cm^2 estimated by Evans and White[36] by using a different method.

Figures 2B-2D, 3 and 4 show the impedance curves for the lithium/BCX cells at increasing storage times of 1, 2, and 3 years, respectively. As can be seen by comparing Fig. 2B-2D, the high frequency loop increases and the low frequency loop disappears with increasing storage time. The steady-state spectrum has a flattened semicircular shape. The centers of the semicircles lie under the real axis of the complex plane. As the storage time increases, the impedance increases as seen in Fig. 3. The centers of the semicircles in Fig. 2 move toward increased charge-transfer resistance, as seen from Fig. 2C and D, and they also move deeper into the imaginary region. This phenomenon can be explained by the statistical distribution of the processes (ionic conduction and charge transfer) occurring at

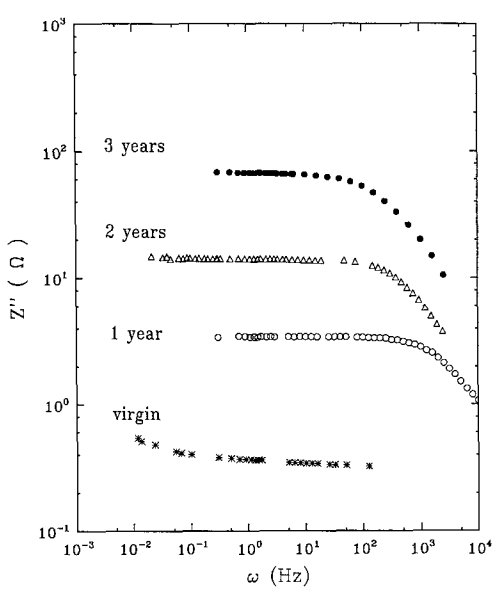

Fig. 3. Bode-magnitude plots of Li/BCX cells at OCV as a function of cell age.

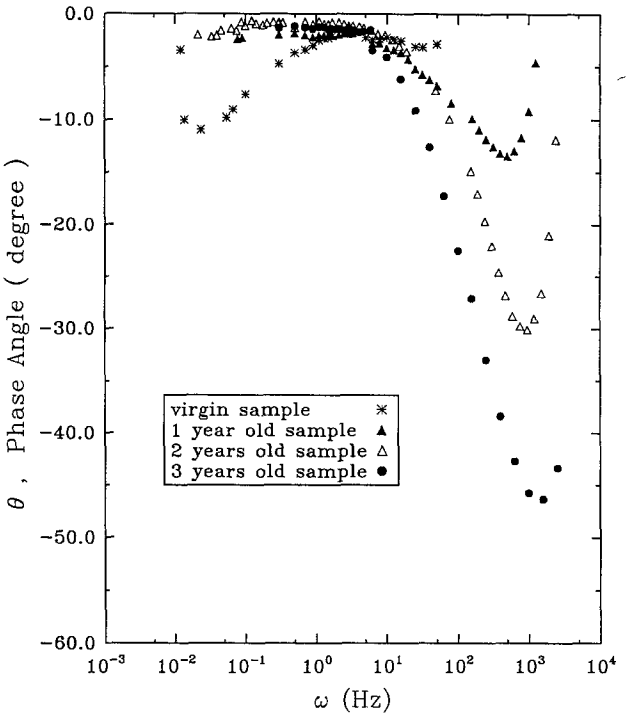

Fig. 4. Bode-phase plots of Li/BCX cells at OCV as a function of cell age.

the bottom of many holes in the surface passive layer.[37] In the presence of a Li passive film the Li self-discharge in $SOCl_2$ is limited by either the ionic or electronic transport through the film. These processes occur independently of each other and depend upon the lattice imperfection in the LiCl passive film and by the potential gradient within the film. As discussed by Delnik,[38] the specific lattice imperfections such as point defects, long-range structural disorder, and impurities, establish the distributions of electronic states and the energies within the bandgap of the passive film. The density of mobile ionic charge carriers (cation vacancies) are also established by the imperfections present in the lattice. As a consequence, the majority charge carriers establish space-charge regions at each interface, provide a mechanism of electron charge injection, and provide a driving force for electronic transport.

For batteries stored 1 year, the equivalent circuit in Fig. 5B provided the best data fit. The elements of this circuit have the following physical meaning: R_1 represents the resistance of the electrolyte in the battery; C_{dl} and R_{ct} represent the double-layer capacitance and the charge-transfer resistance at the metal/solid electrolyte interface, respectively; C_{fil} and R_{fil} correspond to the geometric capacitance and the resistance of the solid electrolyte (SE) interface, respectively. C_{12} and R_{12} correspond to the capacitance of the double layer at the passive film/electrolyte interface and to the transfer resistance of lithium cations across the passive film/electrolyte interface, respectively. This is a modification of the model suggested by Thevenin.[24]

As seen in Fig. 6, the electrolyte resistance, R_1 increases with storage time. The electrolyte resistance as a function of time was computed by fitting the data using the appropriate equivalent circuit given in Fig. 5. These results can be explained by assuming that the pores in the separator are partially blocked by the precipitation of solid LiCl. Hagan and Hampson[39] using gravimetric and spectroscopic methods determined the solubility of LiCl in a 1.8M solution of $LiAlCl_4$ in $SOCl_2$ to be 0.16M. Since the total volume of the electrolyte in Li/BCX D-cell is 2.56×10^{-2} dm^3, the amount of LiCl necessary to saturate the electrolyte is 4.1×10^{-3} moles corresponding to 0.11 Ah or 396 C/mol self-discharge of the battery.

For batteries stored for 3 years as seen in Fig. 2D, a large depressed semicircle with a small "nose" in the low fre-

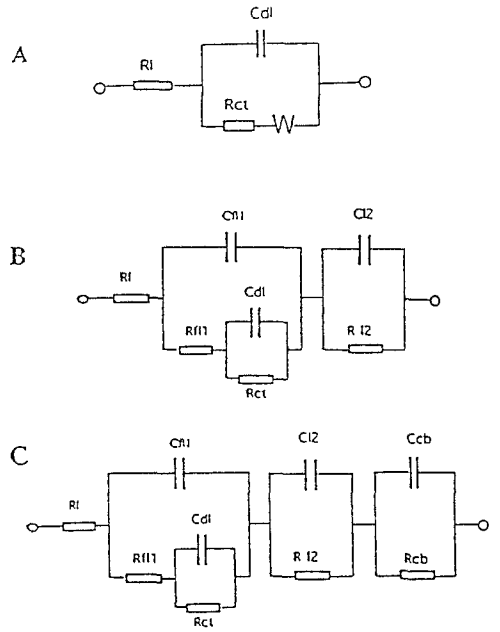

Fig. 5. Equivalent circuits for Li/BCX cells at OCV used for different storage times: A (virgin), B (1 year and 2 years old), C (3 years old).

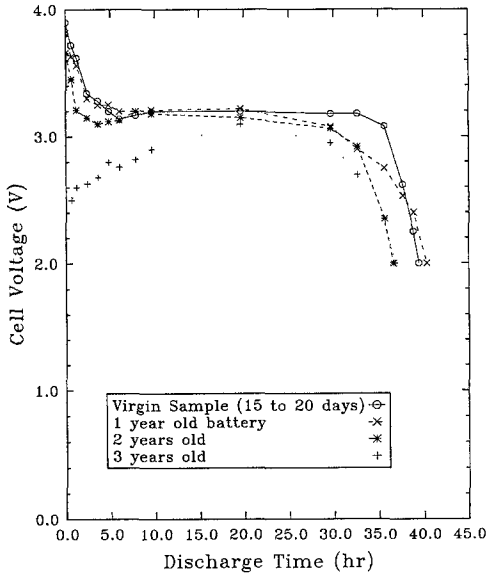

Fig. 7. The entire discharge profiles with a 2 V cutoff voltage. The discharge was carried out at constant resistance of 10 Ω.

quency region is observed. This small arc is due probably to the porous carbon electrode on which lithium chloride has been precipitated. In the low frequency region only a porous carbon electrode with a large effective area and, consequently, a large capacitance value may account for the time constant observed. Thus, the equivalent circuit shown in Fig. 5C accounts for the cathode contributions in the overall impedance spectrum.

To compute the extent of the self-discharge of the cells, virgin batteries (15-20 days old) and batteries 1, 2, and 3 years old were discharged at 0.3 A, using a constant resistance of 10 Ω. The voltage was monitored using a strip chart recorder. Discharge profiles with a 2 V cutoff voltage are presented in Fig. 7. The coulombs of discharge were computed by numerical integration and by averaging the data obtained during testing of four cells stored under identical conditions for each year. Virgin BCX cells stored for 1, 2, and 3 years showed an average self-discharge of 0.95 ± 0.04 Ah (3420 C); 0.81 ± 0.3 Ah (2916 C) and 0.6 Ah ± 0.2 (2160 C) per year, respectively. An average value of 0.95 Ah (3420 C) for self-discharge of 1 year old cells indicates that the concentration of lithium chloride required to saturate

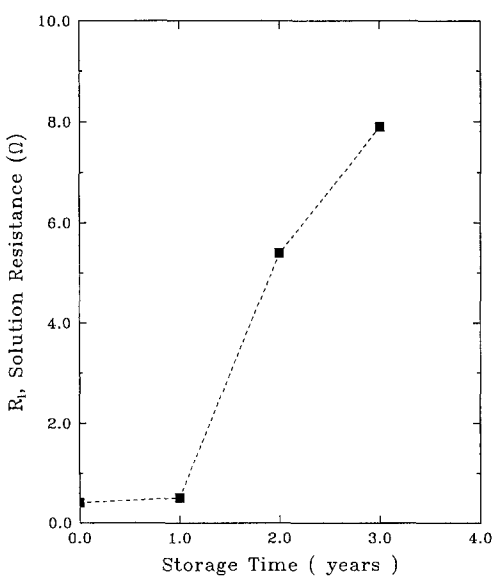

Fig. 6. Dependence of the solution resistance on storage time.

the electrolyte in the cells is attained through Eq. 7 after 1 month of storage. Since the viscosity and the conductivity of the electrolyte in the cell are unchanged when saturated with LiCl, the battery performance should be unaffected. However, the increase in resistivity with time in Fig. 6 can be assumed to be a consequence of electrolyte saturation. The pores in the separator of the battery are partially blocked by the precipitation of solid LiCl. The increased resistivity in the second and third year is probably due to the increased extent of blockage of the pores in the separator or is due to more dense passivating film formed on the separator.

C_{dl} of a virgin cell (15-20 day old) has a value of 1.1 ± 0.8×10^{-3} F. As storage time increases, the double layer capacitance at the metal/film interface decreases as a result of the passivation of the electrode (less electrode active area is available). For batteries stabilized for 1 year a value of $9.3 \pm 2 \times 10^{-6}$ F was observed. Double-layer capacitance values for the metal/film interface in batteries stored for 2 and 3 years were nearly the same. This indicates that the passive film formation on the lithium anode reaches a certain point, and no further changes in the electrode active area occurs. The charge-transfer resistance, R_{ct}, computed for virgin cells has an average value of $5.82 \times 10^{-2} \pm 2.05 \times 10^{-2}$ Ω and increases to a value of $5.34 \times 10^{-2} \pm 1.03 \times 10^{-1}$ Ω for a one year old battery. For batteries stored more than 1 year, the low frequency loop disappears and the Warburg region is no longer observed. Since the polarization resistance is inversely proportional to the active lithium electrode area (the active electrode area decreases as a result of the anode self-discharge), the lithium charge-transfer resistance is expected to increase with storage time.

According to Peled *et al.*,[13-15] the apparent thickness of the passivating film can be calculated by using the equations for a parallel-plate-capacitor

$$C_{fl1} = \frac{\epsilon^o \epsilon_r a}{d} \quad [13]$$

and

$$R_{fl1} = \frac{d}{\sigma a} \quad [14]$$

If the relative permittivity or the conductivity of the passivating film, and its area are known, one can calculate the thickness of the passivating film (d) by using IS to determine the capacitance of the film and by using Eq. 13 or the resistance of the film and by using Eq. 14.

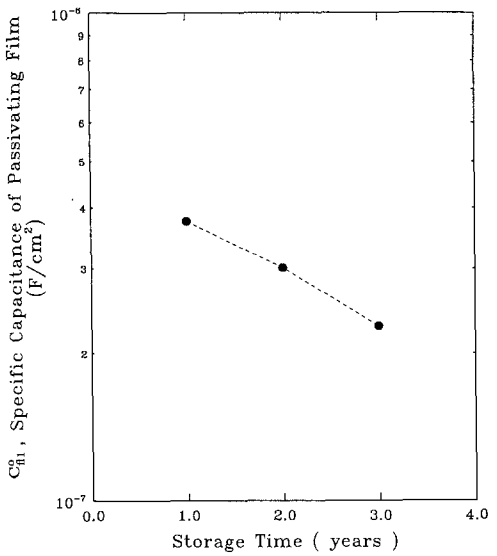

Fig. 8. Dependence of the specific capacitance of the LiCl passivating film, C^a_{fil} on battery storage time.

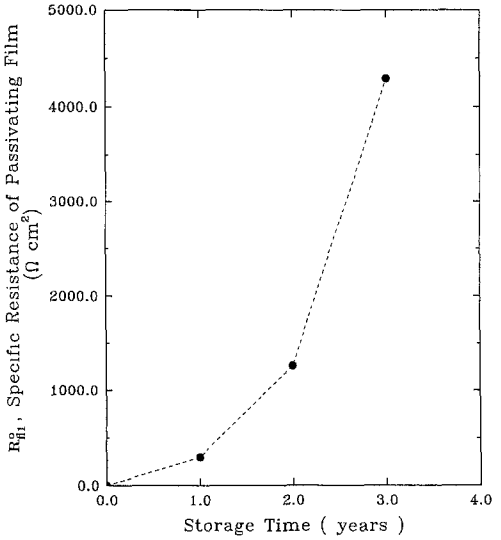

Fig. 9. Dependence of the specific resistance of LiCl passivating film on battery storage time.

Figures 8 and 9 show the dependence of the specific capacitance of the passivating film and the specific resistance of the passivating film, respectively, as a function of storage time. Using a value for conductivity of the solid electrolyte of $\sigma = 5 \times 10^{-9}$ S cm^{-1},[3] and the values of R_{fil} evaluated from the impedance data, the thicknesses of the passivating film were determined as a function of storage time to be 14.7 ± 3 nm in the first year, 63 ± 14 nm the second year, and 214 ± 38 nm for the third year.

For comparison purposes, film thickness data for Li/$LiAlCl_4$-$SOCl_2$ cells as a function of storage time compiled from various references are given in Table. I. As seen in Table I, there are discrepancies between the thicknesses obtained using IS and those obtained by SEM.[16] The thicknesses obtained by IS are smaller than those measured by SEM. Thevenin *et al.*[24] and Holleck *et al.*[40] explained the observed discrepancies by the existence of two or three different sheets of passive layers. The second or the third layers have a polycrystalline structure of LiCl. The second film is porous. Because of the presence of electrolyte in the pores, the second film is not detected by the IS method.

The observed results using IS are in agreement with those obtained from the discharge studies of Li/BCX cells. In Fig. 10, the Li/BCX cell voltage is presented as a function of discharge time at a depth-off-discharge of approximately 2%. The discharge at a rate of 300 mA was performed on virgin batteries (stored 15-20 days) and on batteries 1, 2, and 3 years old. As seen in Fig. 10, at the moment the circuit closes, the voltage falls below its nominal open-circuit potential. The voltage level recovers after a delay time. The transition minimum voltage decreases, and the voltage delay increases with storage time of the battery. The difference between the nominal operating voltage of the cell and the recovered voltage also increases with the increasing storage time. The observed voltage delay is due to the IR drop through the passivating film formed on the anode. As found by IS, the resistivity, density, and thickness of the passivating film increases with storage time thus increases the voltage delay time in Fig. 10. The most severe voltage delay was observed in batteries stored three years. For these batteries, the recovery of the cell voltage takes more that 20 min compared to short recovery times of a few seconds or less for virgin batteries (15-20 days old). The voltage delay is actually the time necessary for the passivating film to deteriorate due to the discharge current. As pointed out by Chenabault *et al.*,[37] during discharge, the transport of the generated lithium ions is hindered by the presence of the passivating layer. As a consequence, a pressure is imposed leading to a physical breakdown of the film. The pressure necessary to break the film is proportional to the density and the thickness of the passivating film and to the magnitude of the discharge current, which, in our case, was kept constant.

For 1 year old Li/BCX cells, the computed thicknesses of the passivating films are an order of magnitude lower than the thickness measured by Meitav and Peled[41] for Li/$SOCl_2$ using the same technique and are 100 times lower than the apparent thickness found using SEM.[16] The presence of BrCl, Br_2, Cl_2, and the BrCl reduction products (see Eq. 2-5) probably cause a change in the morphology and in the composition of the dense passivating film. The small resistivity observed for these batteries indicate that deep cracks are

Table I. The apparent thickness of LiCl passivating film as a function of storage time.

Metal	Electrolyte	Storage time (Days)	Thickness (nm)	Technique	Ref.
Li	$SOCl_2$	1	70	IS[a]	24
Li	$SOCl_2$	3	120	IS	24
Li	$SOCl_2$	16	230	IS	24
Li	$SOCl_2$	36	300	IS	24
Li	$SOCl_2$	93	360	IS	24
Li	$SOCl_2$	125	440	IS	24
Li	$SOCl_2$	1	100-500	IS	13
Li	$SOCl_2$-$LiAlCl_4$	Freshly immersed electrodes	200	IS	43
Li	$SOCl_2$	Freshly immersed electrodes	1000	AES[b]	45
Li	$SOCl_2$	6	1500	GPT[c]	11
Li	$SOCl_2$-$LiAlCl_4$	1	2000-5000	SEM[d]	16

[a] Impedance spectroscopy.
[b] Auger electron spectroscopy.
[c] Galvanostatic pulse technique.
[d] Scanning electron microscopy.

present in the passivating film. Also, the conductivity derived from Eq. 14 is the Li^+ ionic conductivity, which is orders of magnitude above the electronic conductivity.[39] In thin passivating films the space-charge regions near both interfaces overlap. Variation in Li^+ vacancies exist in this area. Consequently the space charge is expected to be significant in thin passivating films because of the large potential difference across the layer (equal to the cell voltage of 3.92 V). At longer storage times, *e.g.*, the observed increase in resistivity of the passivating film is probably due to:

1. The blockage of cracks present in the initial passivating film by precipitation of LiCl crystals.
2. The fact that the space-charge regions separate and include only a small fraction of the passive film which becomes thicker with time.
3. To the presence of BrCl in the electrolyte which probably causes the passivating film to be less ordered and to consist of small crystals resulting in higher concentration of mobile lattice defects. Since the concentration of BrCl in the battery electrolyte decreases at longer storage times due to self-discharge of the battery (see Eq. 7), the passive film of aged batteries consists of large crystals with a higher degree of order, fewer lattice defects, and with less contribution of the grain boundaries to the conduction.
4. The formation of a passivating film on the anode as a result of the presence of sulfur halides, sulfuryl halides, and Br_2 which are formed in partially self-discharged cells according to Eq. 9-11. As suggested by Abraham *et al.*,[22] they may react with the Li anode causing the anode to passivate. Since sulfur halides, sulfuryl halides, and Br_2 are reduction products, their concentration increases at longer storage times in the electrolyte contributing to the film resistivity increase.

It is not possible to determine by using IS which of the mechanisms (the increase of film thickness or the change of the morphology of the film) is responsible for the observed increase in resistivity of the film with storage time.

The variation of the specific double-layer capacitance and the specific charge-transfer resistance at the passivating film/electrolyte interface with storage time are presented in Fig. 11 and 12, respectively. The observed decrease in specific double-layer capacitance at the film/solution interface is probably due to the blockage of the surface of the initial passivating film by LiCl crystals as well as by an increase in the thickness of the double-layer with film growth. The same phenomena was observed by Povarov *et al.*,[42] who studied the impedance of lithium electrodes in thionyl chloride electrolyte for a period of 10 days. Since R_{12} characterizes the process of transfer of lithium ions across the film/electrolyte interface, this parameter should increase with storage time due to the blockage of the compact passivating film/electrolyte interface with LiCl crystals.

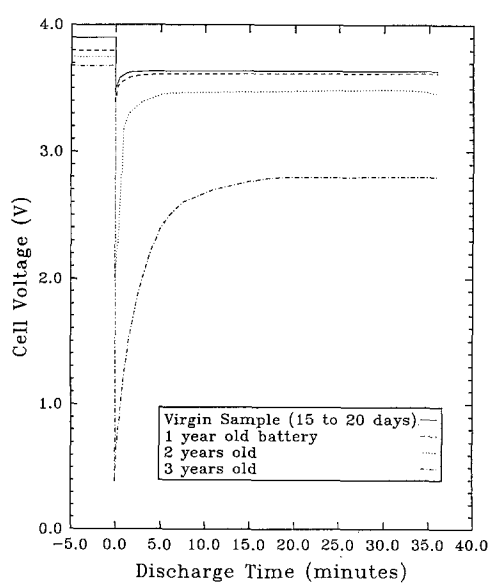

Fig. 10. Discharge behavior of Li/BCX cell at depth-of-discharge close to 2%. The discharge was carried out at constant resistance of 10 Ω and at a current of 300 mA.

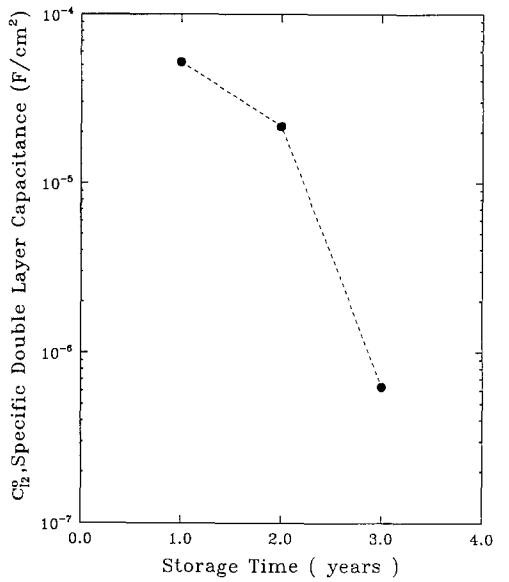

Fig. 11. Dependence of the specific double-layer capacitance, C^o_{12}, of the passivating film/electrolyte interface on storage time.

Conclusions

The purpose of this investigation was to study the growth of LiCl passivating layers on the Li anode in Li/BCX cells. Accordingly, the parameters which characterize the metal/passivating film interphase and passivating film/electrolyte interphase were studied as a function of storage time. The cell impedance was found to be controlled mainly by the anode. The impedance measurements of Li/BCX batteries stored for one to three years showed that the passivating film resistance increases with time because a dense and compact passivating film forms on the anode. The rate of lithium corrosion for virgin cells was estimated to be 0.003 A/cm² and is higher than the average rate of film growth calculated for the first year. This discrepancy is due to the larger Li-exposed area in case of initial Li discharge compared with Li self-discharge in the presence of the passivating film. After discharge, the voltage of the battery

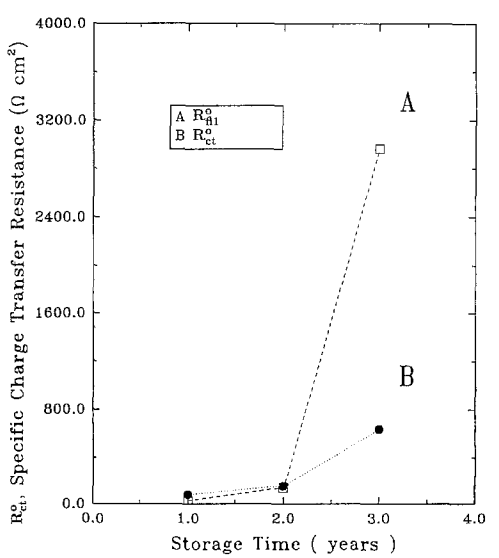

Fig. 12. Relationship between specific charge-transfer resistance and storage time. A, film/electrolyte, R^o_{12}; B; Li anode/film, R^o_{ct}.

immediately falls below its normal open-circuit potential and recovers with a rate which depends on the duration of the storage. The observed transition minimum voltage decreases with the duration of the storage and is due to IR drop on the passivating film. The most severe voltage delay was observed in batteries stored for three years. In order to alleviate this problem a more systematic search for new improved electrolyte compositions for lithium primary batteries is needed.

Acknowledgment

The authors appreciate the financial support of this project by the NASA-Johnson Space Center, Grant No. NAG9-596.

Manuscript submitted Jan. 11, 1993, revised manuscript received June 17, 1993.

The University of South Carolina assisted in meeting the publication costs of this article.

LIST OF SYMBOLS

- a electrode surface area (146 cm^2), cm^2
- C_{dl} double-layer capacitance of Li/solid electrolyte interface, F
- C°_{fil} specific capacitance of the passivating film (C_{fil}/a), F/cm^2
- C_{fil} geometric capacitance of the passivating film, F
- C°_{12} specific double-layer capacitance (C_{12}/a), F/cm^2
- C_{12} double-layer capacitance at the passive film/electrolyte interface, F
- C_{cb} capacitance of carbon cathode, F
- d thickness of the passivating film, cm
- D_i diffusion coefficient of the electroactive species i, cm^2/s
- i_o exchange current density, A/cm^2
- f frequency, Hz.
- F Faraday constant, 96,487 C/mol
- R gas constant, 8.3143 J/mol K
- R_{cb} resistance of carbon cathode, Ω
- R°_{ct} specific charge-transfer resistance (R_{fil}/a), Ω cm^2
- R_{ct} charge-transfer resistance, Ω
- R°_{fil} specific resistance of the passivating film (R_{ct}/a), Ω cm^2
- R_{fil} bulk resistance of the passivating film, Ω
- R_1 resistance of the electrolyte separator, Ω
- R_{12} charge-transfer resistance of lithium cation across the passive film/electrolyte interface, Ω
- T temperature, K
- W Warburg impedance parameter, $\Omega\ cm^2/s^{1/2}$
- Z' real component of impedance, Ω
- Z'' imaginary component of impedance, Ω

Greek

- α dimensionless parameter, a measure of the depression of a semicircle
- ϵ° permittivity in vacuum = 8.85×10^{-14}, F/cm
- ϵ_r the relative permittivity of the solid electrolyte
- θ area of the anode covered by solid electrolyte
- σ conductivity of the solid electrolyte, S/cm
- ω frequency, radians/s, where $\omega = 2\pi f$

REFERENCES

1. M. Mogensen, *J. Power Sources,* **14,** 123 (1985).
2. E. Peled, *This Journal,* **126,** 2047 (1979).
3. M. Mogensen, *J. Power Sources,* **20,** 53 (1987).
4. K. A. Klinedinst and M. J. Domeniconi, *This Journal,* **127,** 1419 (1980).
5. A. N. Dey, *Thin Solid Films,* **43,** 131 (1977).
6. M. J. Harney and S. Brown, Abstract 72, p. 181, The Electrochemical Society Extended Abstracts, Vol. 79-2, Los Angeles, CA, Meeting, Oct. 14-19, 1979.
7. M. Babai and Y. Gal, Abstract 39, p. 106, *ibid.*
8. A. N. Dey, *Electrochim. Acta,* **21,** 21 (1976).
9. J. B. Bailey, *This Journal,* **136,** 2794 (1989).
10. R. V. Moshtev, Y. Geronov, and B. Puresheva, in *Proceedings of 29th ISE Meeting,* Budapest, Vol. 2, p. 818 (Sept. 1978).
11. R. V. Moshtev, Y. Geranov, and B. Puresheva, *This Journal,* **128,** 1851 (1981).
12. D. Chua, W. Merz, and W. Bishop, in *Proceedings of 27th Power Sources Conference,* Atlantic City, New Jersey, June 21-24, 1976, pp. 33-37.
13. E. Peled and H. Yamin, in *Proceedings of the 28th Power Sources Conference,* Atlantic City, NJ, June 12-15, 1978, The Electrochemical Society, Inc., Pennington, NJ, p. 237 (1979).
14. E. Peled, in *Lithium Batteries,* J. P. Gabano, Editor, Chap. 4, Academic Press, Inc., New York (1983).
15. E. Peled and H. Yamin, Izr. *J. Chem.,* **18,** 131 (1979).
16. J. W. Boyd, *This Journal,* **134,** 18 (1987).
17. J. Bressan, Ph.D. Thesis, Universite de Paris (1983).
18. P. W. Krehl and C. Liang, *J. Appl. Electrochem.,* **13,** 431 (1983).
19. C. C. Liang, P. W. Krehl, and D. A. Danner, *ibid.,* **11,** 563 (1981).
20. R. M. Murphy, P. W. Krehl, and C. C. Liang, in *Proceedings of 16th Intersociety Energy Conversion Engineering Conference,* p. 97 (1981).
21. K. M. Abraham and M. Alamgir, *This Journal,* **134,** 2112 (1987).
22. K. M. Abraham, M. Alamgir, and S. J. Perrotti, *ibid.,* **134,** 2112 (1987).
23. E. Darcy, *NASA-JSC Internal Report, JSC-25106* (May 1991).
24. J. Thevenin, *J. Power Sources,* **14,** 45 (1985).
25. G. Monteserelli, P. Nunziante, M. Pasquali, and G. Pistoia, *Solid State Ionics,* **37,** 149 (1990).
26. M. Hughes, S. A. G. R. Karunathilaka, and N. A. Hampson, *J. Appl. Electrochem.,* **14,** 47 (1984).
27. R. V. Moshtev and B. Puresheva, *J. Electroanal. Chem.,* **189,** 609 (1984).
28. N. Matsui, *J. Power Sources,* **20,** 135 (1987).
29. Yu. N. Kuryakov, A. S. Lapa, N. I. Kozlova, T. V. Trofimova, and V. M. Frolov, *Elektrokhimiya,* **26,** 652 (1990).
30. J. Jamnik, M. Gaberscek, and S. Pejovnik, *Electrochim. Acta,* **35,** 423 (1990).
31. M. Gabersscek, J. Jamnik, and S. Pejovnik, *This Journal,* **140,** 308 (1993).
32. M. Hughes, S. A. G. R. Karunathilika, and N. A. Hampson, *J. Appl. Electrochem.,* **13,** 609 (1983).
33. J. R. Macdonald, *J. Electroanal. Chem.,* **131,** 77 (1982).
34. S. A. G. R. Karunathilika, N. A. Hampson, R. Leck, and T. J. Sinclair, *J. Appl. Electrochem.,* **10,** 357 (1980).
35. A. J. Hills, N. A. Hampson, and M. Hayes, *J. Electroanal. Chem,* **209,** 351 (1986).
36. T. I. Evans, T. V. Nguyen, and R. E. White, *This Journal,* **136,** 328 (1989).
37. P. Chenebault, D. Vallin, J. Thevenin, and R. Wiart, *J. Appl. Electrochem.,* **19,** 413 (1989).
38. F. Delnick, *J. Power Sources,* **26,** 129 (1989).
39. W. P. Hagan and N. A. Hampson, *Electrochim. Acta,* **32,** 1787 (1987).
40. G. L. Holleck and K. D. Brady, in *Lithium Batteries,* A. N. Dey, Editor, PV 84-1, p. 48, The Electrochemical Society Proceedings Series, Pennington, NJ (1984).
41. A. Meitav and E. Peled, *J. Electroanal. Chem.,* **134,** 49 (1982).
42. Yu. M. Povarov and V. Vorobeva, *Elektrokhimiya,* **18,** 1693 (1982).
43. R. Keil, J. Hoenigman, W. Modeman, T. Wittberg, and J. Peters, *Interim Techn. Report,* AFWAL-TR-80-2018, University of Dayton Research Institute, Dayton, OH (1979).